



OPEN ACCESS

EDITED BY
Jennifer Sullivan,
Augusta University, United States

REVIEWED BY
Brandi Michele Wynne,
Emory University, United States
Luciana Morla,
INSERM U1138 Centre de Recherche
des Cordeliers (CRC), France

*CORRESPONDENCE
Anita T. Layton,
anita.layton@uwaterloo.ca

SPECIALTY SECTION
This article was submitted to Renal
Physiology and Pathophysiology,
a section of the journal
Frontiers in Physiology

RECEIVED 11 July 2022
ACCEPTED 07 September 2022
PUBLISHED 29 September 2022

CITATION
Stadt MM and Layton AT (2022), Sex and
species differences in epithelial
transport in rat and mouse kidneys:
Modeling and analysis.
Front. Physiol. 13:991705.
doi: 10.3389/fphys.2022.991705

COPYRIGHT
© 2022 Stadt and Layton. This is an
open-access article distributed under
the terms of the [Creative Commons
Attribution License \(CC BY\)](https://creativecommons.org/licenses/by/4.0/). The use,
distribution or reproduction in other
forums is permitted, provided the
original author(s) and the copyright
owner(s) are credited and that the
original publication in this journal is
cited, in accordance with accepted
academic practice. No use, distribution
or reproduction is permitted which does
not comply with these terms.

Sex and species differences in epithelial transport in rat and mouse kidneys: Modeling and analysis

Melissa Maria Stadt¹ and Anita T. Layton^{1,2,3,4*}

¹Department of Applied Mathematics, University of Waterloo, Waterloo, ON, Canada, ²Cheriton School of Computer Science, University of Waterloo, Waterloo, ON, Canada, ³Department of Biology, University of Waterloo, Waterloo, ON, Canada, ⁴School of Pharmacy, University of Waterloo, Waterloo, ON, Canada

The goal of this study was to investigate the functional implications of sex and species differences in the pattern of transporters along nephrons in the rat and mouse kidney, as reported by Veiras et al. (*J Am Soc Nephrol* 28: 3504–3517, 2017). To do so, we developed the first sex-specific computational models of epithelial water and solute transport along the nephrons from male and female mouse kidneys, and conducted simulations along with our published rat models. These models account for the sex differences in the abundance of apical and basolateral transporters, glomerular filtration rate, and tubular dimensions. Model simulations predict that 73% and 57% of filtered Na⁺ is reabsorbed by the proximal tubules of male and female rat kidneys, respectively. Due to their smaller transport area and lower NHE3 activity, the proximal tubules in the mouse kidney reabsorb a significantly smaller fraction of the filtered Na⁺, at 53% in male and only 34% in female. The lower proximal fractional Na⁺ reabsorption in female kidneys of both rat and mouse is due primarily to their smaller transport area, lower Na⁺/H⁺ exchanger activity, and lower claudin-2 abundance, culminating in significantly larger fractional delivery of water and Na⁺ to the downstream nephron segments in female kidneys. Conversely, the female distal nephron exhibits a higher abundance of key Na⁺ transporters, including Na⁺-Cl⁻ cotransporters in both species, epithelial Na⁺ channels for the female rat, and Na⁺-K⁺-Cl⁻ cotransporters for the female mouse. The higher abundance of transporters accounts for the enhanced water and Na⁺ transport along the female rat and mouse distal nephrons, relative to the respective male, resulting in similar urine excretion between the sexes. Model simulations indicate that the sex and species differences in renal transporter patterns may partially explain the experimental observation that, in response to a saline load, the diuretic and natriuretic responses were more rapid in female rats than males, but no significant sex difference was found in mice. These computational models can serve as a valuable tool for analyzing findings from experimental studies conducted in rats and mice, especially those involving genetic modifications.

KEYWORDS

electrolyte transport, homeostasis, pressure natriuresis, renal transporters, saline expansion, water transport

Introduction

The kidneys are among the most essential organs that serve not only as filters, but also play key roles in other essential regulatory functions, including water, electrolyte, and acid-base balance. The regulation of water and electrolyte balance contributes to blood pressure control. Renal transporters play a crucial role in reabsorbing the approximately 1.5 kg of salt that is reabsorbed daily in human kidneys. These transporters include, 1) along the proximal tubules, the apical Na^+/H^+ exchanger 3 (NHE3), 2) along the thick ascending limb of the loop of Henle, the apical $\text{Na}^+-2\text{Cl}^- - \text{K}^+$ cotransport (NKCC2), and 3) along the distal convoluted tubules, the apical Na^+-Cl^- cotransporter (NCC). Along the full nephron, Na^+ transport is driven by the basolateral Na^+-K^+ -ATPase which pumps Na^+ out of the epithelial cells. The final fine-tuning of Na^+ transport is mediated by the collecting duct principal cells via the epithelial Na^+ channel (ENaC) (Palmer and Schnermann, 2015). Dysregulation of these transporters and channels can result in hypo- or hypertension.

Sex differences have long been known in hypertension (Gillis and Sullivan, 2016; Ramirez and Sullivan, 2018). Hence, there is much interest in gaining a better understanding of the mechanisms controlling blood pressure in both sexes. Given the kidney's key role in electrolyte balance and blood pressure regulation, sex differences in hypertension may be attributable, in part, to sex differences in kidney structure and function. Indeed, the renal transporters and channels that mediate electrolyte transport exhibit abundance patterns that are sexually dimorphic, as reported by Veiras et al. (Veiras et al., 2017). Their findings revealed markedly different transport capacity in the proximal tubule of the male and female nephrons of the rat and mouse. Notably, female rat proximal tubules exhibit greater phosphorylated (inactive) NHE3 and re-distribution to the base of the microvilli where activity is lower (Brasen et al., 2014), whereas female mice exhibit a lower NHE3 abundance. In both cases, NHE3 activity is lower in females. Consequently, relative to males, in females the proximal tubule reabsorbs a substantially lower fraction of filtered Na^+ (Veiras et al., 2017). The higher fractional Na^+ distal delivery in females is handled by the augmented transport capacity in the downstream segments. Despite these overall similarities, there are interesting inter-species differences. Proximal tubule apical water permeability is lower in female rat compared to male rat, but higher in female mouse compared to male mouse. While both female rat and mouse exhibit higher abundance of NCC and claudin-7 distal along the distal nephron segments exhibit, female rats also exhibit more abundant ENaC, whereas female mice express more NKCC2 (Veiras et al., 2017).

What are the functional implications of the sexual dimorphism in renal transporter and channel expression patterns in rodents? What are the functional implications of the inter-species differences? To answer the first question for the

rat, we have previously developed sex-specific computational models of solute and water transport along Sprague-Dawley rat nephrons (Li et al., 2018; Hu et al., 2019; Hu et al., 2020), and applied those models to investigate sex differences in kidney function and in responses to pharmacological manipulations (Hu et al., 2021; Swapnasrita et al., 2022). In this study, we developed the first sex-specific computation models for the nephron transport in the C57B16 J mouse kidneys. Using these models, we conduct a comparative study of kidney function in rats and mice. The mouse models in particular can also serve as a valuable tool in better understanding findings in knock-out studies.

Materials and methods

We have previously published epithelial cell-based models of solute and water transport along the nephrons in a rat kidney (Layton et al., 2016a; Layton et al., 2016b). Sex-specific models were formulated to capture the sex differences in morphology, hemodynamics, and transporter patterns in male and female Sprague-Dawley rats. In this study, we developed analogous models for male and female C57B16J mice. We will refer to the models as rat and mouse models, respectively. Model equations (e.g., see Ref. (Layton and Layton, 2018)) are based on mass conservation which are valid for both sexes and across species. Hence, those same equations are used in the mouse models, but appropriate parameter values are changed to account for inter-species and sex differences. The parameter changes for the male and female mouse models versus rats are summarized in Table 1. Each rat kidney model is assumed to contain 36,000 nephrons, whereas each mouse kidney model has 12,000 nephrons.

Model structure

Rodent kidneys consist of multiple types of nephrons; superficial and juxtamedullary nephrons make up most of them (Horster and Thurau, 1968; Jamison, 1973; Haas et al., 1986). In a rat, about two-thirds of the nephron population are superficial nephrons; the loops of Henle of superficial nephrons turn before reaching the inner medulla. The remaining third are called juxtamedullary nephrons. In a mouse, the ratio of superficial-to-juxtamedullary nephron is estimated to be 82:11 (Zhai et al., 2006). The loops of Henle of juxtamedullary nephrons reach into differing depths of the inner medulla. To capture this heterogeneity, we represent six classes of nephrons: a superficial nephron (denoted by "SF") and five juxtamedullary nephrons that are assumed to reach depths of 1, 2, 3, 4, and 5 mm (denoted by "JM-1", "JM-2", "JM-3", "JM-4", and "JM-5", respectively) into the inner medulla. For the rat, the ratios for the six nephron classes are $n_{SF} = 2/3$, $n_{JM-1} = 0.4/3$, $n_{JM-2} = 0.3/3$, $n_{JM-3} = 0.15/3$, $n_{JM-4} = 0.1/3$, and $n_{JM-5} =$

TABLE 1 Key parameter differences between male rat and male mouse nephron models, between male and female rat nephron models, and between male and female mouse nephron models. Rat parameters are taken from published models (Hu et al., 2019; Hu et al., 2020). Mouse parameters are based on data from Refs. (Messow et al., 1980; Veiras et al., 2017; Tahaei et al., 2020; Xu et al., 2021).

Segment	Parameter	Rat M-to-F Δ	Male Rat-to-Mouse Δ	Mouse M-to-F Δ
PT	SNGFR	↓ 20%	↓ 66.7%	↓ 20%
	Plasma [K]	↓ 10%		↓ 7%
	Length/diameter	↓ 20%	↓ 63.6%/20%	↓ 15%
	NHE3 activity	↓ 17%	↓ 32%	↓ 35%
	SGLT2 activity (PCT)	↑ 150%		—
	NaPi activity	↓ 25%		↓ 50%
	Paracellular P _{Na}	↓ 60%		↓ 40%
	Paracellular P _{Cl}	↓ 60%		↓ 40%
SDL	Apical P _f	↓ 36%		↑ 40%
	Length/diameter	↓ 15%	↓ 42.9%/40%	— (Messow et al., 1980)
TAL	Length/diameter	↓ 15%	↓ 35%/10%	— (Messow et al., 1980)
	Na-K-ATPase activity	↑ 100%	↓ 13%	↓ 10%
	NHE activity	↓ 20%		↓ 25%
	NaPi activity	↓ 20%		—
	NKCC2 activity	↑ 100%		↑ 20%
	KCC4 activity	↑ 50%		↑ 64%
	Paracellular P _{Na}	↓ 10%		—
	Paracellular P _{Cl}	↓ 10%		—
DCT	Length/diameter	↓ 15%	↓ 30%/6.7%	— (Messow et al., 1980)
	NCC activity	↑ 100%	↓ 27%	↑ 100%
	Na-K-ATPase activity	↑ 100%	↓ 20%	↑ 25%
	Apical P _K	—	↓ 67%	—
	ENaC activity	↑ 100%	↓ 49%	↑ 17%
	Apical P _f	↑ 100%		↑ 50%
	Paracellular P _{Na}	↑ 40%		↑ 30%
	Paracellular P _{Cl}	↑ 40%		↑ 30%
	NHE activity	↓ 15%		—
	NaPi activity	↓ 15%		—
CNT	Length/diameter	↓ 15%	↓ 60%/16.7%	—
	Apical P _K	—	↓ 75%	—
	H-K-ATPase	—	↓ 50%	—
	Apical P _f	↑ 50%		↑ 20%
	Paracellular P _{Na}	↑ 40%		↑ 30%
	Paracellular P _{Cl}	↑ 40%		↑ 30%
	NHE activity	↓ 10%		—
	NaPi activity	↓ 10%		—
	Na-K-ATPase activity	↑ 100%		—
	ENaC activity	↑ 30%		—
CCD	Length/diameter	↓ 15%	↓ 50%/4%	—
	H-K-ATPase	—	↓ 50%	—
	Apical P _f	↑ 100%		—
	Apical P _K	↓ 30%		—
	Paracellular P _{Na}	↑ 40%		—
	Paracellular P _{Cl}	↑ 40%		—
	NHE activity	↓ 10%		—
	NaPi activity	↓ 10%		—

(Continued on following page)

TABLE 1 (Continued) Key parameter differences between male rat and male mouse nephron models, between male and female rat nephron models, and between male and female mouse nephron models. Rat parameters are taken from published models (Hu et al., 2019; Hu et al., 2020). Mouse parameters are based on data from Refs. (Messow et al., 1980; Veiras et al., 2017; Tahaei et al., 2020; Xu et al., 2021).

Segment	Parameter	Rat M-to-F Δ	Male Rat-to-Mouse Δ	Mouse M-to-F Δ
OMCD	Na-K-ATPase activity	↑ 50%		—
	ENaC activity	↑ 50%		—
	Length/diameter	↓ 15%	↓ 35%/4%	—
	H-K-ATPase	—	↓ 50%	—
	Apical P_f	↑ 100%		—
	Apical P_K	↑ 20%		—
	Apical P_{Na} , P_{Cl}	—		↓ 20%
	NHE activity	↓ 10%		—
	NaPi activity	↓ 10%		—
	Na-K-ATPase activity	↑ 10%		—
IMCD	ENaC activity	↑ 20%		—
	Length/diameter	↓ 15%	↓ 32%/7%	—
	NHE activity	—	↓ 67%	↑ 200%
	Na-K-ATPase activity	↑ 20%	↓ 25%	↑ 20%
	H-K-ATPase activity	↑ 50%	↓ 75%	↑ 50%
	Paracellular P_{Na}	↓ 50%	↓ 33%	↓ 25%
	Apical P_f	↑ 100%		↑ 50%
	Apical P_{Na}	↓ 50%		—
	Apical P_K	↑ 100%		↑ 150%
	Paracellular P_K	—		↑ 200% --
	Paracellular P_{Cl}	↓ 50%		↑ 100% --
	KCC activity	↑ 20%		↑ 300% --
	NKCC activity	↓ 30%		↑ 50%

0.05/3 (Knepper et al., 1977); for the mouse, $n_{SF} = 0.82$, $n_{JM-1} = 0.82 \times 0.4$, $n_{JM-2} = 0.82 \times 0.3$, $n_{JM-3} = 0.82 \times 0.15$, $n_{JM-4} = 0.82 \times 0.1$, and $n_{JM-5} = 0.82 \times 0.05$ (Zhai et al., 2006). The model superficial nephron includes the proximal tubule, short descending limb, thick ascending limb, distal convoluted tubule, and connecting tubule segments. Each of the model juxtamedullary nephrons include all the same segments of the superficial nephron with the addition of the long descending limbs and ascending thin limbs; these are the segments of the loops of Henle that extend into the inner medulla. The length of the long descending limbs and ascending limbs are determined by which type of juxtamedullary nephron is being modeled. The connecting tubules of the five juxtamedullary nephrons and the superficial nephron coalesce into the cortical collecting duct. Single-nephron glomerular filtration rate (SNGFR) for juxtamedullary nephrons is higher than the superficial nephron SNGFR. In rats, the juxtamedullary SNGFR is taken to be 40–50% higher than the superficial SNGFR (Munger and Baylis, 1988; Remuzzi et al., 1988); in mice, the difference is 20%, based on superficial SNGFR and GFR measurements (Messow et al., 1980; Vallon, 2009; Xu et al., 2021).

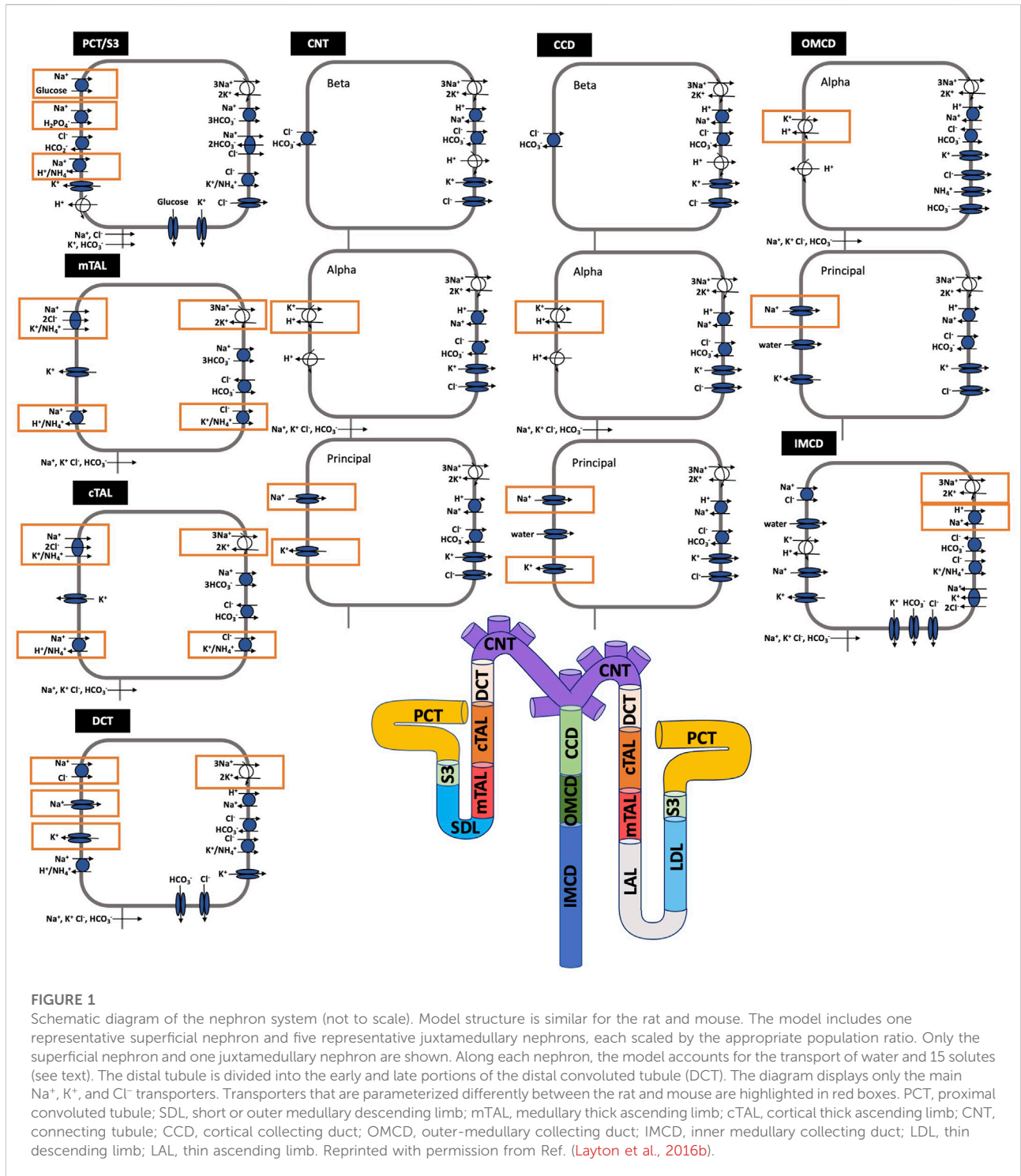
Each nephron segment is modeled as a tubule lined by a layer of epithelial cells in which the apical and basolateral

transporters vary depending on the cell type (i.e., segment, which part of segment, intercalated and principal cells). The model accounts for the following 15 solutes: Na^+ , K^+ , Cl^- , HCO_3^- , H_2CO_3 , CO_2 , NH_3 , NH_4^+ , HPO_4^{2-} , $H_2PO_4^-$, H^+ , HCO_2^- , H_2CO_2 , urea, and glucose. The model consists of a large system of coupled ordinary differential and algebraic equations, solved for steady state, and predicts luminal fluid flow, hydrostatic pressure, membrane potential, luminal and cytosolic solute concentrations, and transcellular and paracellular fluxes through transporters and channels. A schematic diagram of the various cell types, with interspecies differences highlighted, is given in Figure 1.

Model equations

Here we briefly describe the epithelial transport model, which has been described in more detail in Refs. (Layton and Edwards, 2014; Layton et al., 2016b). A schematic diagram of the epithelial transport model and the segments is given in Figure 1.

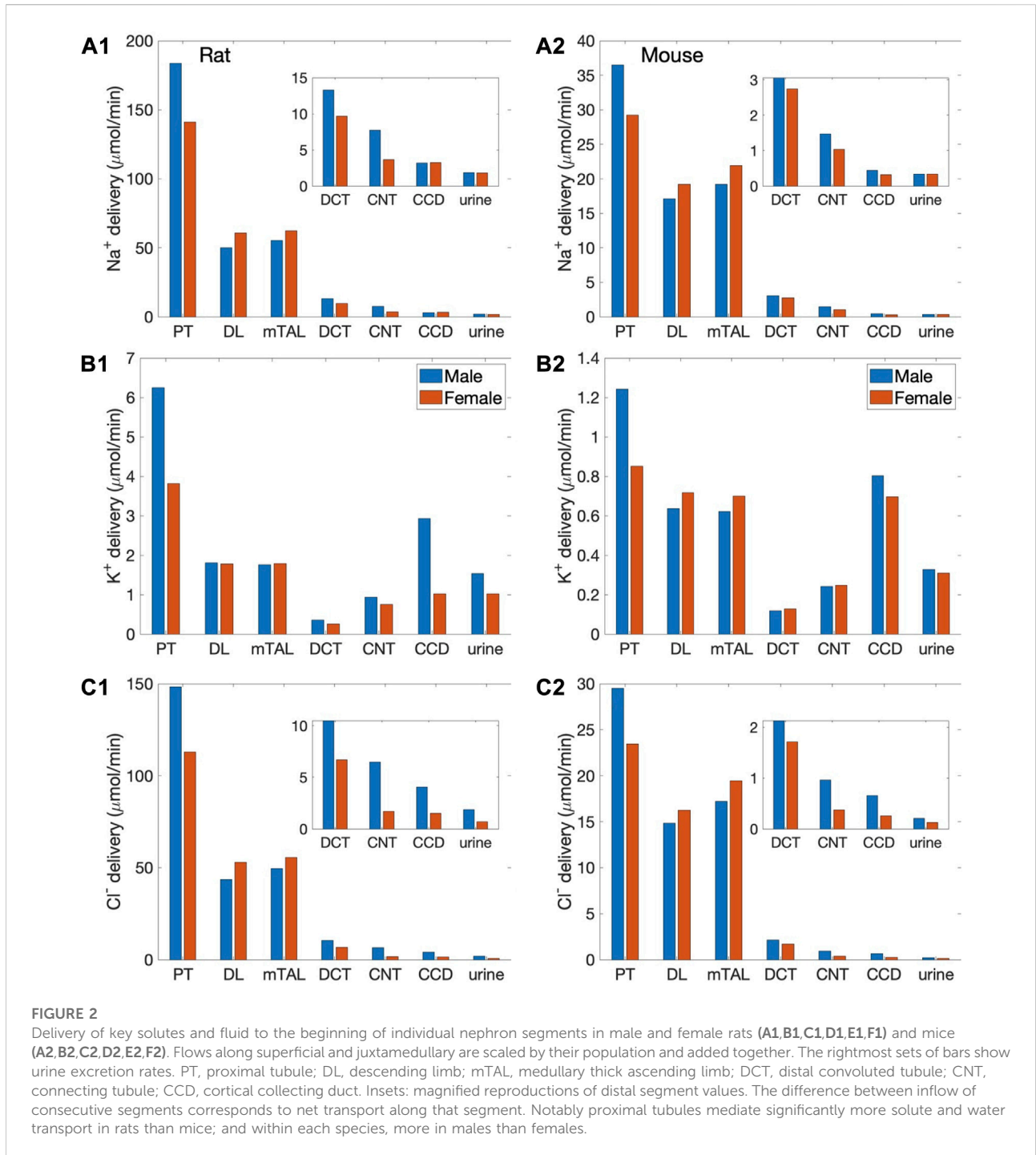
Consider a segment denoted i , ($i = PCT, S3$, etc.) at steady state. For a specific cell along the nephron the cellular,



paracellular, and luminal space are represented by different compartments. Let $J_{v,ab}^i$ denote the transmembrane volume flux from compartment a to compartment b calculated using the osmotic and hydraulic pressure by

$$J_{v,ab}^i = A_{ab}^i L_{p,ab}^i (\sigma_{ab}^i \Delta \pi_{ab}^i + \Delta P_{ab}^i) \quad (1)$$

where A_{ab}^i is the membrane area, $L_{p,ab}^i$ denotes the hydraulic permeability, σ_{ab}^i is the reflection coefficient, $\Delta \pi_{ab}^i = RT \sum \Delta C_{k,ab}^i$, where $\sum \Delta C_{k,ab}^i$ is the osmolality difference, $\Delta C_{k,ab}^i$ denotes the concentration gradient of solute k along the membrane, R the ideal gas constant, T the thermodynamic temperature, and ΔP_{ab}^i is the hydrostatic pressure gradient.



Conservation of volume in the cellular and paracellular compartments (denoted by C and P respectively) is given by

$$J_{v,LC}^i + J_{v,BC}^i + J_{v,PC}^i = 0 \quad (2)$$

$$J_{v,LP}^i + J_{v,BP}^i + J_{v,CP}^i = 0 \quad (3)$$

where L and B denote the lumen and blood, respectively. In the lumen, for non-coalescing segments, conservation of volume is given by

$$\frac{dQ^i}{dx} = 2\pi r^i J_{v,L}^i \quad (4)$$

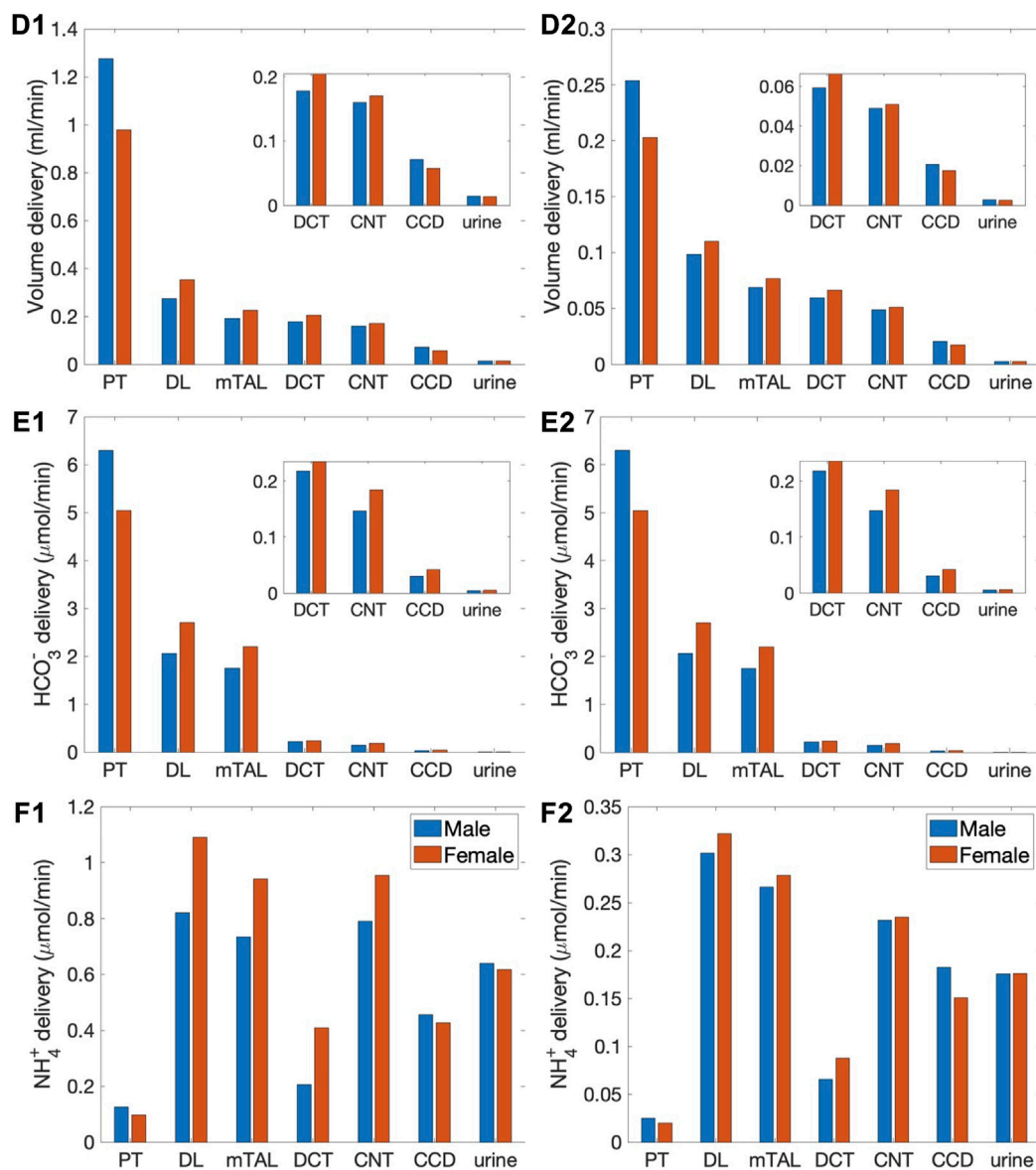


FIGURE 2
 Delivery of key solutes and fluid to the beginning of individual nephron segments in male and female rats (A1, B1, C1, D1, E1, F1) and mice (A2, B2, C2, D2, E2, F2). Flows along superficial and juxtamedullary are scaled by their population and added together. The rightmost sets of bars show urine excretion rates. PT, proximal tubule; DL, descending limb; mTAL, medullary thick ascending limb; DCT, distal convoluted tubule; CNT, connecting tubule; CCD, cortical collecting duct. Insets: magnified reproductions of distal segment values. The difference between inflow of consecutive segments corresponds to net transport along that segment. Notably proximal tubules mediate significantly more solute and water transport in rats than mice; and within each species, more in males than females.

where Q^i denotes the volume flow, r^i is the luminal radius, and $\hat{J}_{v,L}^i \equiv \hat{J}_{v,LC}^i + \hat{J}_{v,LP}^i$ is the total volume flux. The luminal fluid flow is given by pressure-driven Poiseuille flow

$$\frac{dP^i}{dx} = -\frac{8\mu Q^i}{\pi(r^i)^4} \quad (5)$$

where P^i is the hydrostatic pressure and μ is the luminal fluid viscosity.

The luminal radius r^i is assumed to be rigid for all the segments except the proximal tubule (i.e., r^i is constant). Flow-dependent transport for a compliant tubule is assumed along the proximal tubule using the torque-modulated effects approach developed in in Ref. (Weinstein et al., 2007), and described briefly here.

The compliant luminal radius in the proximal tubule (r_{PT}) is given by

TABLE 2 Predicted fraction deliveries and excretions (%) in the rat and mouse nephron models.

	Male rat	Female rat	Male mouse	Female mouse
Late proximal tubule				
Volume	21	36	39	54
Na ⁺	27	43	47	66
K ⁺	29	47	51	84
Late distal convoluted tubule				
Volume	13	17	19	25
Na ⁺	42	26	40	36
K ⁺	15	20	20	29
Urine				
Volume	1.1	1.4	1.1	1.3
Na ⁺	1.0	1.3	0.9	1.1
K ⁺	25	27	26	36

$$r_{PT} = r_{PT}^0 (1 + \mu_{PT} (P_{PT} - P_{PT}^0)) \tag{6}$$

where r_{PT}^0 is the reference radius, P_{PT}^0 is the reference pressure, and μ_{PT} characterizes tubular compliance. In the proximal tubule, transporter density is modulated by luminal flow, so that the microvillous torque is given by

$$\tau_{PT} = \frac{8\mu Q^{PT} l_{PT,mv}}{r_{PT}^2} \left(1 + \frac{l_{PT,mv} + \delta_{PT,mv}}{r_{PT}} + \frac{l_{PT,mv}^2}{2r_{PT}^2} \right) \tag{7}$$

where $l_{PT,mv}$ is the microvillous length and $\delta_{PT,mv}$ denotes the height above the microvillous tip where drag is considered. Using this, we compute

$$S_{torq} = 1 + s \left(\frac{\tau_{PT}}{\tau_{PT}^0} - 1 \right) \tag{8}$$

where τ_{PT}^0 is computed using Eq. 7 with Q^{PT} equal to the initial volume flow at the start of the proximal tubule and r_{PT} as the initial proximal tubule radius, s is a scaling factor. The flux of solutes and volume out of the lumen is then scaled by S_{torq} to capture the torque-modulated effects.

For coalescing segments, i.e., the CNT and IMCD, water and solute flows are scaled by the tubule population where ω^i (for $i = CNT$ or $IMCD$) denotes the fraction of the tubule remaining at a given spatial location where

$$\frac{d}{dx} (\omega^i Q^i) = -2\pi r^i J_{v,L}^i \tag{9}$$

denotes the conservation of volume in the lumen.

The fraction of connecting tubules ω^{CNT} remaining at coordinate x^{CNT} (determined as distance from the start of the connecting tubule) is given by

$$\omega^{CNT} (x^{CNT}) = 2^{-2.32x^{CNT}/L^{CNT}} \tag{10}$$

where L^{CNT} is the connecting tubule length.

The collecting ducts also coalesce in the inner medulla so that the fraction of collecting ducts at distance from the start x^{IMCD} is given by

$$\omega^{IMCD} (x^{IMCD}) = 0.1 \left(1 - 0.95 \left(\frac{x^{IMCD}}{L^{IMCD}} \right)^2 \right) \exp(-2.75x^{IMCD}/L^{IMCD}) \tag{11}$$

where L^{IMCD} is the length of the inner-medullary collecting duct. Eqs. 7, 8 are derived in Ref. (Layton et al., 2016c).

Next, conservation of mass for a non-reacting solutes k in the cellular and paracellular space is given by

$$J_{k,LC}^i + J_{k,BC}^i + J_{k,PC}^i = 0 \tag{12}$$

$$J_{k,LP}^i + J_{k,BP}^i + J_{k,CP}^i = 0 \tag{13}$$

where $J_{k,ab}^i$ denotes the transmembrane flux of solute k from compartment a to compartment b . Unlike transmembrane volume flux ($J_{v,ab}^i$, described above), transmembrane solute flux ($J_{k,ab}^i$) depends on electro diffusion, coupled transport, and primary active transport across ATP-driven pumps. In general, for a solute k across membrane a, b the solute flux $J_{k,ab}^i$ is given by

$$J_{k,ab}^i = (1 - \sigma_{k,ab}^i) \bar{C}_{k,ab}^i J_{v,ab}^i + J_{k,ab}^i (\text{electrodiffusive}) + J_{k,ab}^i (\text{coupled}) + J_{k,ab}^i (\text{ATP-driven}) \tag{14}$$

where the first term represents convective transport, $\sigma_{k,ab}^i$ is the reflection coefficient, and $\bar{C}_{k,ab}^i = (C_{k,a}^i - C_{k,b}^i) / (\ln C_{k,a}^i - \ln C_{k,b}^i)$ is the mean membrane solute concentration. The second term in Eq. 14 denotes the transport via electrodiffusive flux. For ions, electrodiffusive flux is given by the Goldman-Hodgkin-Katz equation

$$J_{k,ab}^i (\text{electrodiffusive}) = h_{k,ab}^i \gamma_{k,ab}^i \left(\frac{C_{k,a}^i - C_{k,b}^i \exp(-\zeta_{k,ab}^i)}{1 - \exp(-\zeta_{k,ab}^i)} \right) \tag{15}$$

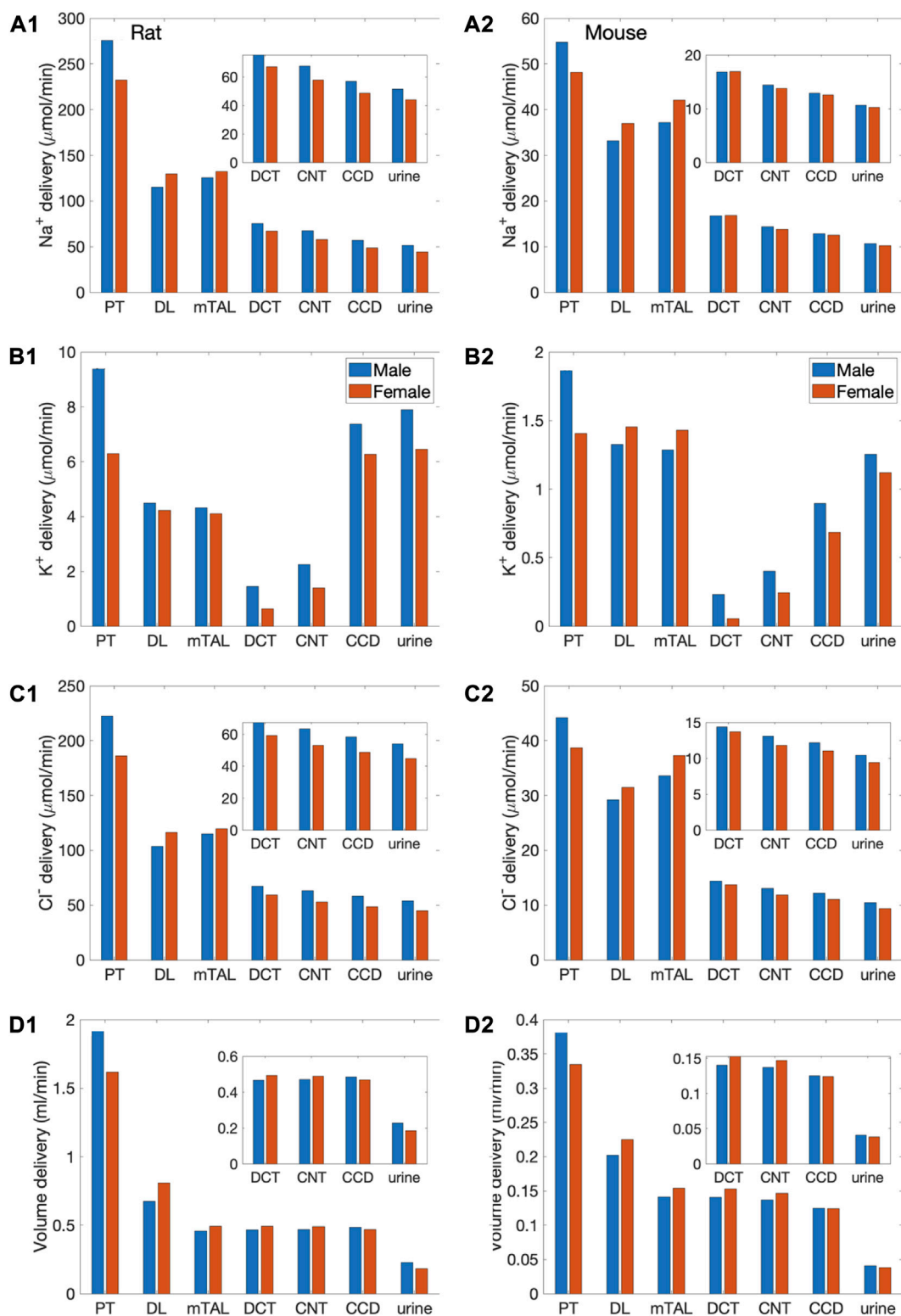


FIGURE 3 Delivery of key solutes and fluid to the beginning of individual nephron segments in male and female rats (A1,B1,C1,D1) and mice (A2,B2,C2,D2) following a saline load. Notations are analogous to Figure 2. Insets: magnified reproductions of distal segment values. The predicted excretion rates are lower for the female models relative to the respective male model. However, when scaled by bolus volume, the female rat model excretes the bolus faster than the male rat model.

where $h_{k,ab}^i$ is the membrane permeability for solute k ,

$$\zeta_{k,ab}^i = \frac{z_k F}{RT} \Delta V_{ab}^i \quad (16)$$

where z_k is the solute valence, F is Faraday's constant, and ΔV_{ab}^i denotes the electrical potential difference. For an uncharged solute, the electrodiffusive flux is given by simple diffusion

$$J_{k,ab}^i (\text{electrodiffusive}) = h_{k,ab}^i (C_{k,a}^i - C_{k,b}^i) \quad (17)$$

since transport does not depend on the electric potential, i.e., only depends on the concentration gradient.

The third term in Eq. 14 denotes the total coupled transport of a solute k across cotransporters and exchangers. The final term in Eq. 14 denotes the total transport via primary active transport (i.e., across ATPases). Transport via cotransporters, exchangers, and primary active transport is determined using existing kinetic models for each transporter (Layton and Edwards, 2014). Figure 1 shows key transporters for the cells of individual segments, with transporters that are parameterized differently between the rat and mouse highlighted.

In the lumen, conservation of non-reacting solutes is given by

$$\frac{d}{dx} (Q^i C_{k,L}^i) = 2\pi r^i \hat{J}_{k,L}^i \quad (18)$$

for non-coalescing segments and

$$\frac{d}{dx} (\omega^i Q^i C_{k,L}^i) = \hat{J}_{k,L}^i \quad (19)$$

for coalescing segments, where $\hat{J}_{k,L}^i \equiv J_{k,LC}^i + J_{k,LP}^i$ denotes the total flux of solute k and ω^i is as defined in Eqs. 10, 11 for the CNT and IMCD respectively.

Conservation is imposed in a similar way on the total buffers for reacting solutes, i.e., acid-base pairs (HPO_4^{2-} , H_2PO_4^-), (NH_3 , NH_4^+) or (HCO_2^- , H_2CO_2). Conservation for reacting solutes is different because of their net generation from reactions. Details on conservation of reacting solutes can be found in Refs. (Chen et al., 2010; Layton and Edwards, 2014).

Results

We simulated nephron transport function for the male and female rats, and the male and female mice. Figure 2 shows the predicted total delivery of key solutes [Na^+ , K^+ , Cl^- , HCO_3^- , and NH_4^+] and fluid to the inlets of individual nephron segments, expressed per kidney, in the four models. Recall that GFR is lower in the female models; thus, solute delivery into the proximal tubules is also lower in females. Note also that plasma [K^+] is lower in female rodents [see Table 1 (Veiras et al., 2017; Li et al., 2019)].

Rats versus mice

The predictions of the rat and mouse nephron models share a number of similarities. Almost all the filtered Na^+ , Cl^- , HCO_3^- , and water is reabsorbed along the nephrons. Most of the Na^+ reabsorption happens along the proximal tubules, via the NHE3, and the thick ascending limbs, via the NKCC2 and Na^+ - K^+ -ATPase. Na^+ transport is accompanied by Cl^- and, along water-permeable segments, by water. The majority of the filtered K^+ is reabsorbed along the proximal tubules and thick ascending limbs. Downstream of Henle's loops, the connecting tubules vigorously secrete K^+ . In the final fine-tuning of K^+ in the luminal fluid, K^+ is reabsorbed along the collecting duct. In both rodent models, the proximal tubule is a major site of NH_4^+ secretion via substitution of H^+ in the NHE3 transporter and secretion of NH_3 . A substantial fraction of NH_4^+ is then reabsorbed along the thick ascending limbs by substituting for K^+ in NKCC2.

The most notable difference between solute handling in the rat and mice is arguably the significantly smaller fraction of filtered Na^+ reabsorbed along the mouse proximal tubules, compared to the rat. This inter-species difference can be attributed to the smaller transport area and lower NHE3 activity in mice. Recall that SNGFR of a superficial mouse nephron is taken to be 1/3 that of a rat (Vallon, 2009). If tubular transport area in the mouse models is also scaled down to 1/3, then taken in isolation, the mouse models would predict urinary excretion rates that are about 1/3 of the corresponding rat models, essentially acting like a smaller rat. The total transport area of a given segment is proportional to the product of its length and diameter. Transport area of the mouse proximal tubule is approximately one-third that of the sex-matched rat. That, together with the lower NHE3 activity (Table 1), results in the mouse proximal tubule transporting a significantly smaller fraction of the filtered Na^+ than rat in both sexes. The rat proximal tubules are predicted to reabsorb 73% and 57% of the filtered Na^+ in the male and female models, respectively. In contrast, the male proximal tubules reabsorbed only 53% of the filtered Na^+ ; the female proximal tubules even less, only 34%. Consequently, downstream segments in mice must handle a larger fraction of the filtered Na^+ . In particular, the thick ascending limbs mediate 44% of the filtered Na^+ in male mouse and 64% in female, significantly more than the 23% in male rat and 37% in female rat. Since Na^+ transport drives the reabsorption of Cl^- and water, and other electrolytes similar inter-species difference is also seen in the segmental transport of water and other solutes; see Figure 2.

Further comparison can be found in the fractional delivery and excretion rates of water, Na^+ , and K^+ , which are summarized in Table 2. Predictions for the rat models have been previously validated (Layton et al., 2016b; Hu et al., 2019). Predictions for the male mouse model are consistent with micropuncture data (Wulff et al., 2002; Loffing et al., 2004; Vallon et al., 2005).

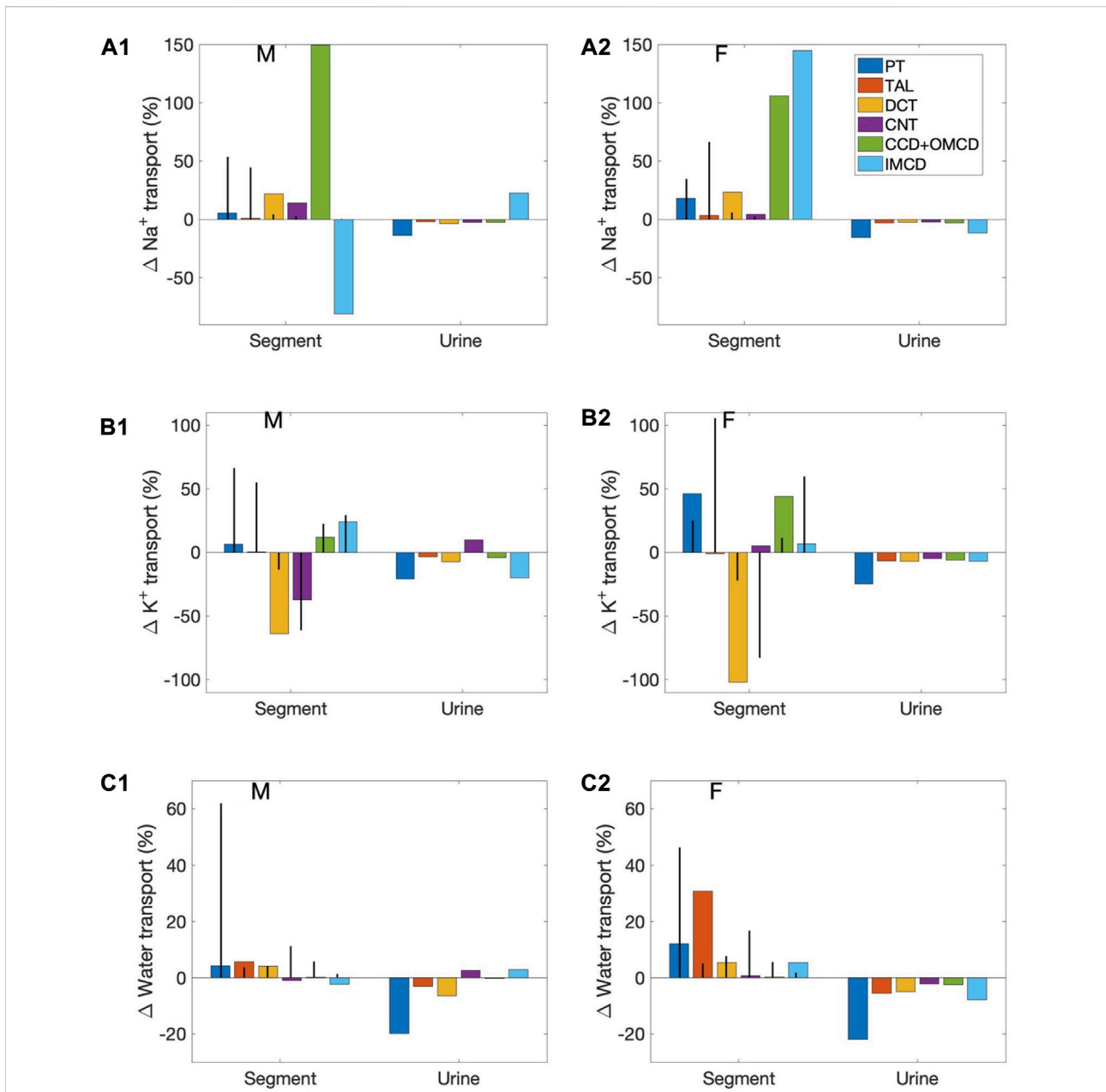


FIGURE 4
 Effects on segmental transport and urine excretion if transporter abundance in individual segments was set to values in the sex-matched rat. Results show 1) fractional changes in Na^+ transport (A1, A2), K^+ transport (B1, B2), and water transport (C1, C2) along each nephron segment in the male mouse (A1, B1, C1) and female mouse (A2, B2, C2) if transporter abundance in individual segments were set to values in the sex-matched rat, and 2) Na^+ excretion, K^+ excretion, and urine output. Six segments were considered individually: proximal tubule (PT), thick ascending limb (TAL), distal convoluted tubule (DCT), connecting tubule (CNT), cortical and outer-medullary collecting ducts (CCD + OMCD), and inner-medullary collecting duct (IMCD). Middle bars (vertical lines) indicate fractional transport mediated by that segment under baseline conditions.

Males versus females

The sexual dimorphisms in renal transporters in rats and mice exhibit similarities as well as differences. In both species, the abundance of key transporters in the proximal tubules is lower in females. Notably, there are fewer NHE3 overall in female mice,

and more phosphorylated (inactive) NHE3 in female rat, both of which implies lower NHE3 activity in females. The abundance of claudin-2 is also lower both females. One notable difference between the two species is the sex differences in proximal tubule AQP1 expression, which is 40% higher in female mice compared to males, but 60% lower in female rats. These differences in

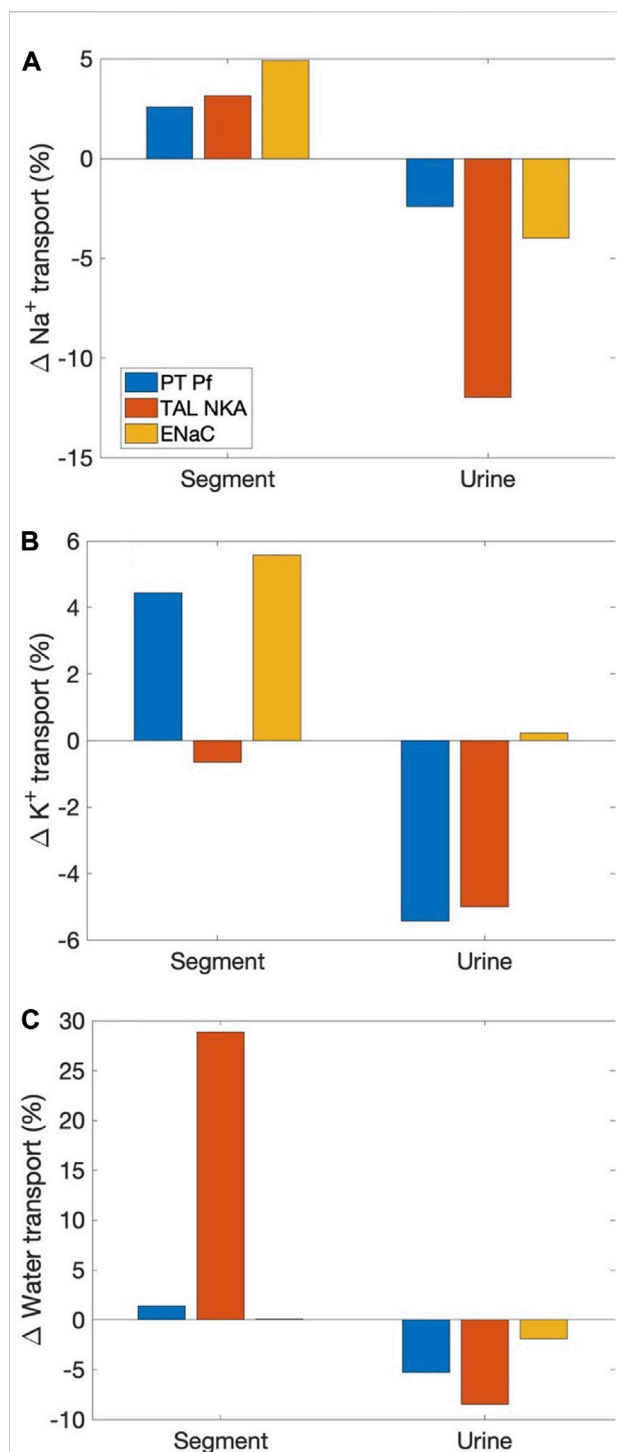


FIGURE 5

Effects on segmental transport and urinary excretion in the female mouse if selected sex differences in mice were changed to corresponding differences in the rat. Three sex differences that are most qualitatively different between the two species were considered: 1) proximal tubule apical water permeability ("PT Pf"), 2) thick ascending limb Na^+ - K^+ -ATPase ("TAL NKA"), and 3) ENaC. Results show fractional changes in Na^+ transport (A), K^+ transport (B), and water transport (C) along affected segments, as well as the corresponding changes in urinary excretion rates and volume.

proximal transporter abundance are represented in the model; see Table 1. The lower NHE3 activity in females appear to have the most dominating effect: the models predict that a larger fraction of the filtered Na^+ is reabsorbed in the male species relative to females, as noted above. Because water transport is driven by Na^+ reabsorption, even though the female mouse expression more AQP1, a significantly larger fraction of the filtered volume is reabsorbed along the proximal tubules in the male mouse (61%) compared to female (46%).

The resulting proportionally higher Na^+ load and volume in females is handled by the distal segments, which express a higher abundance of key transporters, including more NKCC2, NCC, and claudin-7 in mice, and more ENaC, NCC, ENaC, and claudin-7 in rats. These sex differences are represented by setting appropriate transport parameter values in the models; see Table 1.

Responses to Na^+ load

Veiras et al. (Veiras et al., 2020) reported that the response to an acute Na^+ load differs between rats and mice, and between the two sexes. Specifically, given the same saline bolus volume relative to body weight, diuretic and natriuretic responses were more rapid in female rats, with the fractional excretion of the bolus more than twice in female rats compared to males at 3 h. In contrast, no significant difference was found between the excretion rates of male and female mice. We conducted simulations to determine whether the baseline model transport parameters would predict a similar sex difference in rats, and no difference in mice. To simulate a saline load, we increase SNGFR by 50% in the male rat and mouse models (Cervenka et al., 1999; Blantz et al., 2012), and by 65% in the female rat and mouse models, to take into account the greater salt-loading induced increases in macula densa NOS1 β expression and activity in females than in males (Zhang et al., 2020). All other parameters remained unchanged.

The model predicts some degree of glomerulotubular balance in all four models, with proximal tubular Na^+ transport increases in response to the higher Na^+ load (Figure 3). Water and Cl^- transport primarily follows Na^+ ; the model predicts significant increases in proximal tubular water and Cl^- reabsorption in all models (Figure 3). Despite the enhanced proximal reabsorption, Na^+ delivery to the thick ascending limb is about twice the baseline values. Consequently, Na^+ reabsorption along the thick ascending limb is also predicted to increase. Na^+ load is predicted to substantially impact K^+ transport along the thick ascending limb and connecting tubule. K^+ reabsorption approximately doubles along the thick ascending limb, whereas K^+ secretion along the connecting tubule is predicted to increase markedly (Figure 3).

Taken together, the above transport processes result in urine flow of 241 and 194 $\mu\text{L}/\text{min}$, respectively, in male and female rats,

and 41 and 38 $\mu\text{L}/\text{min}$, respectively, in male and female mice, given per kidney. Urinary Na^+ excretion is predicted to be 54 and 47 $\mu\text{mol}/\text{min}$, respectively, for each male and female rat kidney, and 11 and 10 $\mu\text{mol}/\text{min}$, respectively, for each male and female mouse kidney. Assuming that a female rat weighs about one-half that of the male rat (at 10–12 weeks, [Envigo.com](https://www.envigo.com)), then the saline bolus volume simulated in the female model is one-half that of the male model. Thus, the female-to-male ratio of Na^+ excretion (denoted E_{Na}) as a fraction of saline load is given by $(\text{female } E_{\text{Na}}/\text{male } E_{\text{Na}})/(\text{female saline volume}/\text{male saline volume}) = (47/54)/0.5 = 1.74$. A mature male C56BL/6 mouse weighs approximately 30% more than an age-matched female (16 weeks; the Jackson Laboratory). The analogous ratio for mice is given by $(10/11) \times 1.3 = 1.18$. Thus, the model predicts an interesting inter-species difference: that female rats excrete a saline load significantly faster than male rats, whereas male and female mice had more similar responses. That result is consistent with findings by Veiras et al. ([Veiras et al., 2020](https://doi.org/10.1016/j.kintp.2020.100000)). Similarly, the female-to-male ratios of fractional volume excretion are predicted to be significantly higher for rats (1.58) than for mice (1.20).

Segmental contributions to inter-species differences in nephron transport

Segmental contributions to interspecies differences in nephron transport. As previously noted, between the rat and the mouse, there are notable differences in the fractional solute and water transport by individual nephron segments. These differences are found in both males and females, and are a result of the differences in transporter patterns of the two species. To understand the functional implications of these inter-species differences, we first conducted simulations to study how differences in transporter patterns of individual segments affect solute and water transport along those segments, as well as urinary excretion. Specifically, we set the transporter and channel activities of individual nephron segments of the mouse model to the corresponding rat values (of the same sex), and computed the resulting changes in segmental transport and urinary excretion. Six “segments” were considered: 1) proximal convoluted and straight tubules, 2) medullary and cortical thick ascending limbs, 3) distal convoluted tubule, 4) connecting tubule, 5) cortical and outer-medullary collecting duct, and 6) inner-medullary collecting duct. Only transporter and channel activities were modified, but not other parameters such as SNGFR and segmental lengths and diameters. For example, for the proximal tubule simulations, NHE3 activity along the proximal convoluted and straight tubules in the mouse models was increased by 47% to agree with the rat values (to eliminate the 32% difference between rat and mouse; see [Table 1](https://doi.org/10.3389/fphys.2022.991705)). That would be the only change. We then computed how this change affects solute and water transport along the proximal tubule, separately for male and female, as well as urinary excretion rates. The differences relative to baseline are

shown in [Figure 4](https://doi.org/10.3389/fphys.2022.991705) as blue bars (labelled “PT”). Solute and water transport was also affected along other segments downstream, but those differences are not shown. Consider the connecting tubule as another example. To eliminate the species differences for this segment, apical K^+ permeability and $\text{H}^+-\text{K}^+-\text{ATPase}$ were increased (see [Table 1](https://doi.org/10.3389/fphys.2022.991705)). New simulation results were compared with baseline to determine the effects on solute and water transport along the connecting tubule, and on urinary excretion, and displayed as purple bars in [Figure 4](https://doi.org/10.3389/fphys.2022.991705) (labelled “CNT”).

First consider the left group of bars in [Figure 4](https://doi.org/10.3389/fphys.2022.991705) (labelled “Segment”), which show percentage changes in Na^+ , K^+ , and water transport along each mouse nephron segment if its transporter abundance were the same as a sex-matched rat. The 6 bars in each group correspond to separate simulations in which transport properties were varied in different segments, as explained above. These results answer the question: *How do these inter-species differences affect transport along that particular segment?* However, due to the large differences in fractional transport among segments (e.g., under baseline conditions, the proximal tubules of the male mouse reabsorb almost 20 times more Na^+ transport the cortical and outer-medullary collecting ducts), these percentage changes do not translate directly into absolute changes, and cannot be compared between segments. Also, transport along downstream segments was also affected (results not shown). To assess impacts on overall kidney function, resulting changes in Na^+ excretion, K^+ excretion, and urine volume are also included in [Figure 4](https://doi.org/10.3389/fphys.2022.991705). These results answer the question: *How do mouse-specific transporter activity values along individual segments impact overall transport?*

Changes in the proximal tubules and inner-medullary collecting ducts have the largest effect on urinary excretions and output. In the mouse proximal tubule, NHE3 is downregulated compared to the rat. If a mouse proximal tubule exhibits the same NHE3 activity as a sex-matched rat, proximal tubule transport would significantly elevate and, despite some compensation along downstream segments, Na^+ excretion, K^+ excretion, and urine output would all decrease by up to 20%. Changes in the proximal tubules have a large effect on nephron function because, except in the female mouse (more below), the proximal tubules via the NHE3 mediate the majority of Na^+ transport. In the female mouse, most of the filtered Na^+ is reabsorbed by the thick ascending limbs. However, the difference in thick ascending limb transporter abundance between the rat and mouse is small, only a 13% reduction in $\text{Na}^+-\text{K}^+-\text{ATPase}$ activity. When $\text{Na}^+-\text{K}^+-\text{ATPase}$ activity along the thick ascending limbs is increased to rat level, the models predict only minor reductions in Na^+ excretion, K^+ excretion, and urine output.

Changes in the inner-medullary collecting duct also have a large effect on nephron function even though that segment is responsible for only a minute fraction of overall nephron transport because a number of transporter parameters are assumed to be different between the rat and the mouse (NHE3, $\text{Na}^+-\text{K}^+-\text{ATPase}$, and $\text{H}^+-\text{K}^+-\text{ATPase}$ activities as well as paracellular Na^+

permeability), and, perhaps more importantly, it is the last segment with no downstream segments to compensate. These changes have competing effects on electrolyte and water transport. Thus, the net effects on urinary excretions and output depends on the solute and sex. See [Figure 4](#).

A closer look at sex differences in the rat versus mouse nephron

Sexual dimorphism in transport pattern is qualitatively similar between the rat and mouse, except for a few transporters. Based on the immunoblotting results by Veiras et al. (Veiras et al., 2020), the present models assume 1) proximal tubule apical water permeability (P_f) is lower in female rat compared to male rat, but higher in female mouse compared to male mouse; 2) Na^+ - K^+ -ATPase activity is doubled in female rat from males along the thick ascending limbs, distal convoluted tubules, and connecting tubules, but the analogous sex difference is much smaller in mice; 3) ENaC activity is assumed to be significantly higher in female rat relative to male, but there is no sex difference in mice. See [Table 1](#). *What are the function implications of these inter-species differences in sex differences?* To answer that question, we conducted three simulations, in which selective sex differences in the mouse models were made rat-like. Specifically, 1) proximal tubule P_f in the female mouse was set to 36% lower than male mouse like the rats (instead of 40% higher); 2) Na^+ - K^+ -ATPase activity along the thick ascending limbs, distal convoluted tubules, and connecting tubules in female mouse is set to twice the male mouse values (instead of small to no change); 3) ENaC activity along the connecting tubules, cortical and outer-medullary collecting ducts of the female mouse is set to 30%, 50%, and 20%, respectively, above male values (instead of no difference).

As expected, all these changes increased Na^+ reabsorption along the affected segments; see [Figure 5](#). Water transport increased as well. Note that while the percentage increase in water transport for the “thick ascending limb Na^+ - K^+ -ATPase activity” case is nearly 30%, the net increase is small because the thick ascending limbs are nearly water impermeable. K^+ transport increased as well, except when thick ascending limb Na^+ - K^+ -ATPase activity was increased, which limits K^+ reabsorption along the thick ascending limbs. All changes suppressed urinary Na^+ and K^+ excretion and urine output, except when ENaC activity is increased. That modification increases K^+ secretion and excretion.

Discussion

Physiology is fascinating in its many layers of complexity. Even within a species, one finds that the structures and

functions of organ and tissue systems may be affected by a multitude of factors, including sex and gender, age, time of day or year, and race or strain. The present study analyzes kidney function along two dimensions, sex and species. To accomplish that goal, we developed and applied sex-specific computational models for nephron transport in the rat and mouse kidney. The models represent the sexual dimorphism in renal morphology, hemodynamics, and transporter abundance (Munger and Baylis, 1988; Veiras et al., 2017). Model simulations were conducted to compare kidney function between the rat and mouse, between males and females.

Before discussing the physiological insights gleaned from the simulation results, we note that a notable contribution of this study is the development of epithelial transport models of the mouse kidney. The mouse is the animal model used in over 95% of animal studies, given its small size and the similarity it shares with human's genome (99%). Genetically modified mouse models have been essential for understanding physiological mechanisms, as well as the pathogenesis, progression, and treatments of diseases. Genetically manipulated animals almost always develop compensatory response, which can muddle the results. To help distinguish response to the intended genetic manipulation from compensation, computational models can be used to simulate “clean” genetic modification experiments. However, while most of the genetic modification animal models are mice, computational models of the mammalian kidney have been focused on the rat, because of the more abundant morphological, electrochemical, and micropuncture data. Recently, analogous computational models were developed for humans, for their higher and more relevant clinical value, despite the sparsity of measurements needed to determine model parameters. In contrast, no such models exist, until now, for the mouse. In the absence of a mouse computational model, theoretical analysis was often performed using a rat model to explain experimental observations made in mouse studies [e.g., (Layton et al., 2016; Layton and Vallon, 2018; Wei et al., 2018)]. That is, clearly, less than ideal, given the plentiful inter-species differences in morphology, hemodynamics, and molecular structure, some of which have been discussed in this study. The mouse nephron models developed in this study finally allows us to supplement genetically modified mouse kidney experiments with *in silico* studies using computational models of the mouse kidney. Recognizing that sex is a key biological variable, the mouse nephron models, like their rat counterparts, are sex specific. Thus, not only do these mouse models yield relevant and accurate predictions for both sexes, but they can also be used to extrapolate experimental findings obtained in one sex to the other.

Another goal of this study is to understand the physiological implications of the differences in renal transporter distribution between female and male nephrons. Both the rat and mouse nephrons exhibit lower Na^+ and water transporters and lower fractional reabsorption in the proximal nephrons of females versus males, coupled with more abundant transporters in

renal tubule segments downstream of the macula densa (Veiras et al., 2017). Fine control of Na^+ excretion, important in the regulation of body electrolyte, volume, and blood pressure, is accomplished by the tight regulation of Na^+ transport along the distal tubular segments (Greger, 2000). Hence, the larger contribution of the distal nephron segments to total renal Na^+ transport in females may better equip them for the fluid and electrolyte retention and adaptations demanded of them during pregnancy and lactation. Results of our recent modeling studies (Stadt and Layton, 2022) suggest that the female renal transporter pattern, together with the pregnancy-induced adaptations, make possible the fluid, Na^+ , and K^+ retention required for a healthy pregnancy. Those models were formulated for a rat in mid- and late pregnancy. Extending the model to a pregnant mouse, when the necessary transporter expression data become available, might shed light into how the female mouse transporter abundance pattern, despite its differences from that of the female rat, would also meet the enhanced fluid and electrolyte demands in pregnancy.

Notwithstanding the similarities in the sex differences in transporter abundance patterns in the rat and mouse nephrons, there are notable differences in the transporters along the proximal tubules (AQP1) and distal segments (NKCC2, Na^+ - K^+ -ATPase, and ENaC) between rats and mice. These interspecies differences may provide a partial explanation for the two rodents' different response to an acute Na^+ load. Veiras et al. (Veiras et al., 2017) reported that female rats excrete an acute Na^+ load faster than male rats. Specifically, given the same saline bolus volume relative to body weight, diuretic and natriuretic responses were more rapid in female rats, with female rats excreting ~30% and male rats <15% of the saline bolus at 3 h. In contrast, no significant difference was observed between the male and female mice. That difference in the rat versus mouse response is likely not fully explained by the discrepancies in their baseline kidney structure and function, as an acute saline load will likely trigger alternations in renal transporter expression, which have not been measured separately for each sex and are thus not incorporated in the present simulations. Furthermore, extrarenal systems that participate in the pressure-natriuresis response, such as the renin-angiotensin system, exhibit differences between the two species and between sexes. Thus, a full understanding of each species' sex-specific response to a saline load and other hypertensive stimuli requires a more comprehensive computational model [e.g., (Ahmed and Layton, 2019; Leete and Layton, 2019)]. Given that the kidney maintains the balance of not only Na^+ but other electrolytes and acid-base, it would be interesting to better characterize any sex dimorphisms in the two species' response to K^+ load or other stimuli [e.g., (Harris et al., 2019)] the differs significantly, and if that can be explained by differences in their transporter abundance patterns.

It is our hope that our computational kidney models can be a useful tool in synthesizing and analyzing the large amount

of data emerging from different experimental studies. The ultimate goal is to utilize *in silico* studies to advance our understanding of kidney physiology and pathophysiology, and support therapeutic drug development. With that goal in mind, limitations of the present models must be acknowledged. They include the paucity of experimental data at the cellular level, the limited availability of direct measurements of transport activities and membrane permeabilities, and the lack of explicit representation of intracellular signaling pathways (Weinstein, 2003; Layton and Edwards, 2014). Also, the present models assume that the interstitial fluid composition is known *a priori*, thereby ignoring the interactions of nephron segments are not represented. This limitation can be overcome by updating the interstitial fluid concentrations using basolateral fluxes, using an approach similar to Refs. (Layton and Layton, 2003; Fry et al., 2015). Furthermore, as noted above, kidney function is modulated not only by sex but many other factors as well. For instance, numerous physiological functions exhibit circadian oscillations (Patke et al., 2020), and the kidney is no exception. Renal plasma flow, GFR, and tubular reabsorption and/or secretion processes have been shown to peak during the active phase and decline during the inactive phase (Costello et al., 2022). Interestingly, but perhaps not surprisingly, the circadian regulation of renal transporter expression level exhibits sex difference (Crislip et al., 2020). Incorporating circadian regulation of filtration and transport into the computational models, expanding upon what was done for an isolated proximal tubule cell model (Wei et al., 2018), would make for more chronologically accurate predictions of kidney function, and provide a new tool for chronopharmacological studies. Another worthwhile extension is the simulation of Na^+ inhibitors, including furosemide, to understand any differences between the responses in male and female mice, as was done using the rat models (Layton et al., 2016a; Hu et al., 2020).

Data availability statement

Publicly available datasets were analyzed in this study. This data can be found here: <https://github.com/Layton-Lab/nephron>.

Author contributions

AL: conceptualization, methodology, visualization, resources, data curation, supervision, project administration, and funding acquisition. AL and MS: software, validation, formal analysis, investigation, writing—original draft preparation, writing—review and editing, read, and agreed to the submitted version of the manuscript.

Funding

This research was supported by the Canada 150 Research Chair program and by the Natural Sciences and Engineering Research Council of Canada, *via* a Discovery award (RGPIN-2019-03916) to AL.

Conflict of interest

The authors declare that the research was conducted in the absence of any commercial or financial relationships that could be construed as a potential conflict of interest.

References

- Ahmed, S., and Layton, A. T. (2019). Sex-specific computational models for blood pressure regulation in the rat. *Am. J. Physiol. Ren. Physiol.* 318, F888–F900. doi:10.1152/ajprenal.00376.2019
- Blantz, R. C., Singh, P., Deng, A., Thomson, S. C., and Vallon, V. (2012). Acute saline expansion increases nephron filtration and distal flow rate but maintains tubuloglomerular feedback responsiveness: role of adenosine A(1) receptors. *Am. J. Physiol. Ren. Physiol.* 303, F405–F411. doi:10.1152/ajprenal.00329.2011
- Brasen, J. C., Burford, J. L., McDonough, A. A., Holstein-Rathlou, N. H., and Peti-Peterdi, J. (2014). Local pH domains regulate NHE3-mediated Na⁺ reabsorption in the renal proximal tubule. *Am. J. Physiol. Ren. Physiol.* 307, F1249–F1262. doi:10.1152/ajprenal.00174.2014
- Cervenka, L., Mitchell, K. D., and Navar, L. G. (1999). Renal function in mice: effects of volume expansion and angiotensin II. *J. Am. Soc. Nephrol.* 10, 2631–2636. doi:10.1681/ASN.V10122631
- Chen, J., Edwards, A., and Layton, A. T. (2010). Effects of pH and medullary blood flow on oxygen transport and sodium reabsorption in the rat outer medulla. *Am. J. Physiol. Ren. Physiol.* 298, F1369–F1383. doi:10.1152/ajprenal.00572.2009
- Costello, H. M., Johnston, J. G., Juffre, A., Crislip, G. R., and Gumz, M. L. (2022). Circadian clocks of the kidney: Function, mechanism, and regulation. *Physiol. Rev.* 102, 1669–1701. doi:10.1152/physrev.00045.2021
- Crislip, G. R., Douma, L. G., Masten, S. H., Cheng, K.-Y., Lynch, I. J., Johnston, J. G., et al. (2020). Differences in renal BMAL1 contribution to Na⁺ homeostasis and blood pressure control in male and female mice. *Am. J. Physiol. Ren. Physiol.* 318, F1463–F1477. doi:10.1152/ajprenal.00014.2020
- Fry, B. C., Edwards, A., and Layton, A. T. (2015). Impacts of nitric oxide and superoxide on renal medullary oxygen transport and urine concentration. *Am. J. Physiol. Ren. Physiol.* 308, F967–F980. doi:10.1152/ajprenal.00600.2014
- Gillis, E. E., and Sullivan, J. C. (2016). Sex differences in hypertension: Recent advances. *Hypertension* 68, 1322–1327. doi:10.1161/HYPERTENSIONAHA.116.06602
- Greger, R. (2000). Physiology of renal sodium transport. *Am. J. Med. Sci.* 319, 51–62. doi:10.1097/0000441-200001000-00005
- Haas, J., Granger, J., and Knox, F. (1986). Effect of renal perfusion pressure on sodium reabsorption from proximal tubules of superficial and deep nephrons. *Am. J. Physiol.* 250, F425–F429. doi:10.1152/ajprenal.1986.250.3.F425
- Harris, A. N., Lee, H.-W., Fang, L., Verlander, J. W., and Weiner, I. D. (2019). Differences in acidosis-stimulated renal ammonia metabolism in the male and female kidney. *Am. J. Physiol. Ren. Physiol.* 317, F890–F905. doi:10.1152/ajprenal.00244.2019
- Horster, M., and Thurnau, K. (1968). Micropuncture studies on the filtration rate of single superficial and juxtamedullary glomeruli in the rat kidney. *Pflügers Arch. Gesamte Physiol. Menschen Tiere* 301, 162–181. doi:10.1007/BF00362733
- Hu, R., McDonough, A. A., and Layton, A. T. (2019). Functional implications of the sex differences in transporter abundance along the rat nephron: modeling and analysis. *Am. J. Physiol. Ren. Physiol.* 317, F1462–F1474. doi:10.1152/ajprenal.00352.2019
- Hu, R., McDonough, A. A., and Layton, A. T. (2020). Sex-differences in solute transport along the nephrons: Effects of Na⁺ transport inhibition. *Am. J. Physiol. Ren. Physiol.* 319, F487–F505. doi:10.1152/ajprenal.00240.2020
- Hu, R., McDonough, A. A., and Layton, A. T. (2021). Sex differences in solute and water handling in the human kidney: Modeling and functional implications. *PLoS Comput. Biol.* 24, 102667. doi:10.1016/j.isci.2021.102667
- Jamison, R. L. (1973). Intrarenal heterogeneity: The case for two functionally dissimilar populations of nephrons in the mammalian kidney. *Am. J. Med.* 54, 281–289. doi:10.1016/0002-9343(73)90022-3
- Knepper, M. A., Danielson, R. A., Saidel, G. M., and Post, R. S. (1977). Quantitative analysis of renal medullary anatomy in rats and rabbits. *Kidney Int.* 12, 313–323. doi:10.1038/ki.1977.118
- Layton, A. T., and Edwards, A. (2014). *Mathematical modeling in renal physiology*. Germany: Springer.
- Layton, A. T., and Layton, H. E. (2003). A region-based model framework for the rat urine concentrating mechanism. *Bull. Math. Biol.* 65, 859–901. doi:10.1016/S0092-8240(03)00045-4
- Layton, A. T., and Layton, H. E. (2018). A computational model of epithelial solute and water transport along a human nephron. *PLoS Comput. Biol.* 15, e1006108. doi:10.1371/journal.pcbi.1006108
- Layton, A. T., and Vallon, V. (2018). SGLT2 inhibition in a kidney with reduced nephron number: Modeling and analysis of solute transport and metabolism. *Am. J. Physiol. Ren. Physiol.* 314, F969–F984. doi:10.1152/ajprenal.00551.2017
- Layton, A. T., Laghmani, K., Vallon, V., and Edwards, A. (2016a). Solute transport and oxygen consumption along the nephrons: effects of Na⁺ transport inhibitors. *Am. J. Physiol. Ren. Physiol.* 311, F1217–F1229. doi:10.1152/ajprenal.00294.2016
- Layton, A. T., Vallon, V., and Edwards, A. (2016b). A computational model for simulating solute transport and oxygen consumption along the nephrons. *Am. J. Physiol. Ren. Physiol.* 311, F1378–F1390. doi:10.1152/ajprenal.00293.2016
- Layton, A. T., Vallon, V., and Edwards, A. (2016c). Predicted consequences of diabetes and SGLT inhibition on transport and oxygen consumption along a rat nephron. *Am. J. Physiol. Ren. Physiol.* 310, F1269–F1283. doi:10.1152/ajprenal.00543.2015
- Leete, J., and Layton, A. T. (2019). Sex-specific long-term blood pressure regulation: Modeling and analysis. *Comput. Biol. Med.* 104, 139–148. doi:10.1016/j.combiomed.2018.11.002
- Li, Q., McDonough, A. A., Layton, H. E., and Layton, A. T. (2018). Functional implications of sexual dimorphism of transporter patterns along the rat proximal tubule: modeling and analysis. *Am. J. Physiol. Ren. Physiol.* 315, F692–F700. doi:10.1152/ajprenal.00171.2018
- Li, J., Xu, S., Yang, L., Yang, J., Wang, C. J., Weinstein, A. M., et al. (2019). Sex difference in kidney electrolyte transport II: impact of K⁺ intake on thiazide-sensitive cation excretion in male and female mice. *Am. J. Physiol. Ren. Physiol.* 317, F967–F977. doi:10.1152/ajprenal.00125.2019
- Loffing, J., Vallon, V., Loffing-Cueni, D., Aregger, F., Richter, K., Pietri, L., et al. (2004). Altered renal distal tubule structure and renal Na⁺ and Ca²⁺ handling in a mouse model for Gitelman's syndrome. *J. Am. Soc. Nephrol.* 15, 2276–2288. doi:10.1097/01.ASN.0000138234.18569.63
- Messow, C., Gärtner, K., Hackbarth, H., Kangaloo, M., and Lünebrink, L. (1980). Sex differences in kidney morphology and glomerular filtration rate in mice. *Contrib. Nephrol.* 19, 51–55.

The handling editor JS declared a past co-authorship with the author AL.

Publisher's note

All claims expressed in this article are solely those of the authors and do not necessarily represent those of their affiliated organizations, or those of the publisher, the editors and the reviewers. Any product that may be evaluated in this article, or claim that may be made by its manufacturer, is not guaranteed or endorsed by the publisher.

- Munger, K., and Baylis, C. (1988). Sex differences in renal hemodynamics in rats. *Am. J. Physiol.* 254, F223–F231. doi:10.1152/ajprenal.1988.254.2.F223
- Palmer, L. G., and Schnermann, J. (2015). Integrated control of Na transport along the nephron. *Clin. J. Am. Soc. Nephrol.* 10, 676–687. doi:10.2215/CJN.12391213
- Patke, A., Young, M. W., and Axelrod, S. (2020). Molecular mechanisms and physiological importance of circadian rhythms. *Nat. Rev. Mol. Cell Biol.* 21, 67–84. doi:10.1038/s41580-019-0179-2
- Ramirez, L. A., and Sullivan, J. C. (2018). Sex differences in hypertension: where we have been and where we are going. *Am. J. Hypertens.* 31, 1247–1254. doi:10.1093/ajh/hpy148
- Remuzzi, A., Puntorieri, S., Mazzoleni, A., and Remuzzi, G. (1988). Sex related differences in glomerular ultrafiltration and proteinuria in munich-wistar rats. *Kidney Int.* 34, 481–486. doi:10.1038/ki.1988.206
- Stadt, M. M., and Layton, A. T. (2022). Adaptive changes in single-nephron GFR, tubular morphology, and transport in a pregnant rat nephron: modeling and analysis. *Am. J. Physiol. Ren. Physiol.* 322, F121–F137. doi:10.1152/ajprenal.00264.2021
- Swapnasrita, S., Carlier, A., and Layton, A. T. (2022). Sex-specific computational models of kidney function in patients with diabetes. *Front. Physiol.* 14, 741121. doi:10.3389/fphys.2022.741121
- Tahaei, E., Coleman, R., Saritas, T., Ellison, D. H., and Welling, P. A. (2020). Distal convoluted tubule sexual dimorphism revealed by advanced 3D imaging. *Am. J. Physiol. Ren. Physiol.* 319, F754–F764. doi:10.1152/ajprenal.00441.2020
- Vallon, V., Grahmmer, F., Volkl, H., Sandu, C. D., Richter, K., Rexhepaj, R., et al. (2005). KCNQ1-dependent transport in renal and gastrointestinal epithelia. *Proc. Natl. Acad. Sci. U. S. A.* 102, 17864–17869. doi:10.1073/pnas.0505860102
- Vallon, V. (2009). Micropuncturing the nephron. *Pflugers Arch.* 458, 189–201. doi:10.1007/s00424-008-0581-7
- Veiras, L. C., Girardi, A. C. C., Curry, J., Pei, L., Ralph, D. L., Tran, A., et al. (2017). Sexual dimorphic pattern of renal transporters and electrolyte homeostasis. *J. Am. Soc. Nephrol.* 28, 3504–3517. doi:10.1681/ASN.2017030295
- Veiras, L. C., McFarlin, B. E., Ralph, D. L., Buncha, V., Prescott, J., Shirvani, B. S., et al. (2020). Electrolyte and transporter responses to angiotensin II induced hypertension in female and male rats and mice. *Acta Physiol.* 229, e13448. doi:10.1111/apha.13448
- Wei, N., Gumz, M. L., and Layton, A. T. (2018). Predicted effect of circadian clock modulation of NHE3 of a proximal tubule cell on sodium transport. *Am. J. Physiol. Ren. Physiol.* 315, F665–F676. doi:10.1152/ajprenal.00008.2018
- Weinstein, A. M., Weinbaum, S., Duan, Y., Du, Z., Yan, Q., and Wang, T. (2007). Flow-dependent transport in a mathematical model of rat proximal tubule. *Am. J. Physiol. Ren. Physiol.* 292, F1164–F1181. doi:10.1152/ajprenal.00392.2006
- Weinstein, A. M. (2003). Mathematical models of renal fluid and electrolyte transport: acknowledging our uncertainty. *Am. J. Physiol. Ren. Physiol.* 284, F871–F884. doi:10.1152/ajprenal.00330.2002
- Wulff, P., Vallon, V., Huang, D. Y., Völkl, H., Yu, F., Richter, K., et al. (2002). Impaired renal Na⁺ retention in the sgk1-knockout mouse. *J. Clin. Invest.* 110, 1263–1268. doi:10.1172/JCI15696
- Xu, S., Li, J., Yang, L., Wang, C. J., Liu, T., Weinstein, A. M., et al. (2021). Sex difference in kidney electrolyte transport III: Impact of low K intake on thiazide-sensitive cation excretion in male and female mice. *Pflugers Arch.* 473, 1749–1760. doi:10.1007/s00424-021-02611-5
- Zhai, X.-Y., Thomsen, J. S., Birn, H., Kristoffersen, I. B., Andreasen, A., and Christensen, E. I. (2006). Three-dimensional reconstruction of the mouse nephron. *J. Am. Soc. Nephrol.* 17, 77–88. doi:10.1681/ASN.2005080796
- Zhang, J., Zhu, J., Wei, J., Jiang, S., Xu, L., Qu, L., et al. (2020). New mechanism for the sex differences in salt-sensitive hypertension: the role of macula densa NOS1 β -mediated tubuloglomerular feedback. *Hypertension* 75, 449–457. doi:10.1161/HYPERTENSIONAHA.119.13822